Simultaneous targeting of TIRAP and RIPK2: An effective approach for the treatment of chronic inflammatory diseases

M.Sc. Thesis

By

AYUSHI

DEPARTMENT OF BIOSCIENCES AND BIOMEDICAL ENGINEERING

INDIAN INSTITUTE OF TECHNOLOGY INDORE

MAY 2025

Simultaneous targeting of TIRAP and RIPK2: An effective approach for the treatment of chronic inflammatory diseases

A THESIS

Submitted in partial fulfillment of the
requirements for the award of the degree

of
Master of Science

by
AYUSHI

DEPARTMENT OF BIOSCIENCES AND BIOMEDICAL ENGINEERING
INDIAN INSTITUTE OF TECHNOLOGY INDORE

MAY 2025

INDIAN INSTITUTE OF TECHNOLOGY INDORE

CANDIDATE'S DECLARATION

I hereby certify that the work which is being presented in the thesis entitled "**Simultaneous targeting of TIRAP and RIPK2: An effective approach for the treatment of chronic inflammatory diseases**" in the partial fulfillment of the requirements for the award of the degree of **MASTER OF SCIENCE** and submitted in the **DEPARTMENT OF BIOSCIENCES AND BIOMEDICAL ENGINEERING, IIT Indore**, is an authentic record of my own work carried out during the period from July 2024 to May 2025 under the supervision of Dr Mirza S. Baig, Professor, Department of Biosciences and Biomedical Engineering.

The matter presented in this thesis has not been submitted by me for the award of any other degree of this or any other institute.

Ayushi 23/05/25

Signature of the student with date

AYUSHI

This is to certify that the above statement made by the candidate is correct to the best of my/our knowledge.

Signature of the Supervisor of M.Sc. thesis

Dr. Mirza S. Baig

AYUSHI has successfully given his/her M.Sc. Oral Examination held on **5th May 2025**.

Signature of Supervisor of MSc thesis

Date: 05/05/2025

Convener, DPGC

23-05-2025

ACKNOWLEDGEMENTS

This thesis is more than a culmination of academic effort- it is the reflection of a journey filled with challenges, learning, growth, and immense gratitude. As I look back on this transformative phase of my life, I am overwhelmed with appreciation for those who have guided, supported, and inspired me along my way.

First and foremost, I extend my deepest and sincerest gratitude to my supervisor, **Prof. Mirza Saqib Baig**, for his unwavering support and invaluable guidance throughout my master's thesis. His encouraging nature and constructive criticism provided direction during times of doubt. I extend my sincere gratitude to the Head and DPGC Convener of the Discipline of BSBE and Course coordinator for their continuous support and encouragement. The faculty members of BSBE have been instrumental in broadening my understanding of research concepts, and I am thankful for their insightful guidance.

Special thanks are due to **Mr. Lateefur Rahman Khan, Mr. Gaurav Singh, Mr. Arif Patel**, for their invaluable assistance and support in the laboratory. I would especially like to thank **Dr. Ravinder** for his valuable discussions and generous time at SIC facility of IIT Indore.

A special note of appreciation is reserved for my lab mates, who became more than just colleagues- MSB lab family. I am happy to extend my heartfelt gratitude to **Rajat Atre**, my mentor. I thank **Kundan Solanki, Khandu Wadhonkar, Pramod Patidar, Sk Rameej Raja, Krishma Bajaj, Shreya Bharti, Anil Prajapati, Shubham Kumar Behera, Faaiza Siddiqi** and **Rigzin Yangdol** for their unprecedented advice during the crucial phases of my master's thesis.

I owe the deepest gratitude to my family-my parents, **Mr. Braj Mohan** and **Mrs. Manju**, my younger brother **Yuvraj**, and extended gratitude to **Mrs. Poonam**, **Mr. Rattandeep**, and **Aryan** for their unconditional love,

unwavering support, and constant encouragement. Their belief in me has been my greatest motivation. This journey would not have been possible without their silent sacrifices and endless blessings. I am also grateful to my friends and classmates for their unwavering support and encouragement throughout my academic journey. Lastly, I express my gratitude to the **Almighty** for blessing me with the health, strength, and perseverance needed to carry this journey through to completion.

Dedicated to My Parents

Mr. Braj Mohan, Mrs. Manju,

my sibling Yuvraj

and my Family

Abstract

Chronic inflammation is a prolonged immune response characterized by the persistent activation of immune cells, leading to tissue damage and the development of various diseases, including cancer, cardiovascular disorders, and autoimmune conditions. Macrophages play a central role in chronic inflammation by producing pro-inflammatory cytokines and mediating the immune response to infections. In bacterial infection-associated chronic inflammation, key signaling pathways involving RIPK2 and TIRAP are activated. RIPK2 is a critical mediator downstream of receptors recognizing Gram-positive bacteria. Its activation triggers NF-κB and MAPK pathways, which results in the production of inflammatory cytokines. Similarly, TIRAP acts as an adaptor protein in the Toll-like receptor (TLR) signaling pathway, which detects bacterial components of Gram-negative bacteria. TIRAP facilitates the recruitment of downstream signaling molecules, amplifying the inflammatory response. Given their central roles in modulating immune responses, targeting both RIPK2 and TIRAP offers a promising therapeutic approach to mitigate chronic inflammation associated with bacterial infections. Inhibiting these pathways can effectively suppress the excessive production of pro-inflammatory cytokines, thereby reducing inflammation caused by both Gram-positive and Gram-negative bacteria. This dual-target strategy has the potential to provide a broad-spectrum therapeutic solution for treating bacterial infection-induced chronic inflammatory diseases.

LIST OF PUBLICATIONS

1. Tomokazu Ohishi, Sayaka Yuki; Junjiro Yoshida, Daisuke Tatsuda, Manabu Kawada, Akiko Shiraishi; Faaiza Siddiqi; **Ayushi Yadav; Mirza Baig**, Akira Yano ***" Amacha, a Japanese sweet tea made from Hydrangea macrophylla var. thunbergii, inhibits infection by pseudolentiviruses expressing the SARS-CoV-2 spike protein" : Food Chemistry Advances*** *(Under Revision)* (Manuscript Number: **FOODCHEM-D-24-13556)**
2. Rigzin Yangdol, **Ayushi Yadav**, and **Mirza S Baig**, ***"TIRAP in Cancer: A New Frontier"*** (Under preparation)
3. Sk Rameej Raja, Mobassar Hassan Sk V, Syed Wajeed, Rigzin Yangdol, **Ayushi Yadav**, Himanshi Jindal, Arif Siddiquie, Ramachandran Subramanian, **Mirza S Baig** , "***Macrophage Transcriptional Dynamics During Acute and Chronic wound Repair"*** (Submitted)

TABLE OF CONTENTS

LIST OF FIGURES

LIST OF TABLES

NOMENCLATURE

BTK: Bruton's Tyrosine Kinase

DAMPs: Damage-Associated Molecular Patterns

NOD: Nucleotide-binding and oligomerization domain

IL-1β: Interleukin-1β

IL-6: Interleukin-6

IMPPAT: Indian Medicinal Plants, Phytochemistry and Therapeutics

PAMPs: Pathogen-Associated Molecular Patterns

PKCδ: Protein Kinase C Delta

PRR: Pattern Recognition Receptor

RA: Rheumatoid Arthritis

TIRAP: Toll/IL-1 Receptor Domain Containing Adaptor Protein

TNF α: Tumor Necrosis Factor-Alpha

WS: *Withania somnifera*

Chapter 1: Introduction

1.1 Inflammation

Inflammation is a complex response of the host's immune system to harmful stimuli, such as pathogens (bacteria and viruses, etc.), damaged cells, and certain irritants such as silica dust. It is a protective response involving a complex interplay of immune cells, signaling mediators, and physiological changes that aims to eventually eliminate the cause of the injury, clear out the damaged tissue, and initiate the healing process [1]. Vasodilation increases vascular permeability, and local blood flow alterations are hallmark features of inflammation. These changes are orchestrated by mediators such as histamine, prostaglandins, and bradykinin. Vasodilation allows for increased blood supply to the affected area, while increased vascular permeability enables immune cells and plasma proteins to extravasate into the tissue, leading to the characteristic redness and swelling seen in inflammation. The initiation of inflammation is typically triggered by the recognition of PAMPs or DAMPs by PRRs on immune and certain non-immune cells, including dendritic, epithelial cells, and macrophages[2]. This recognition sets off a series of intracellular signaling pathways, leading to the production of pro-inflammatory cytokines like TNF-α, IL-1β, and IL-6. Neutrophils, monocytes, and macrophages are the primary cellular players in the inflammatory response. Neutrophils are the primary cells to arrive at the infection/injury site, phagocytosing pathogens and releasing antimicrobial agents[3]. Monocytes migrate to the site and differentiate into macrophages, which clear cellular debris and release growth factors to aid tissue repair. Additionally, lymphocytes, including T cells and B cells, participate in regulating the immune response and maintaining immune memory. When the inflammatory response persists beyond its intended purpose, chronic inflammation can develop. This condition is associated with various diseases, such as atherosclerosis, RA, and certain cancers.

Chronic inflammation often involves a dysregulated immune response and the continuous release of pro-inflammatory mediators[4]. The initiation as well as resolution of inflammation are highly regulated events, and dysregulation in this inflammatory signaling often results in persistent inflammation. Triggered by stimuli, the uncontrolled host immune cell-mediated inflammation leads to the proinflammatory cytokine storm, which results in increased inflammatory mediators and inflammatory cells for pathogen control. When there is an imbalance between anti-inflammatory and pro-inflammatory responses, it can result in damage to tissue, vascular dysfunction, multi-organ failure, and ultimately death in many instances. Various molecules, including macrophages, play a major role in mediating the inflammatory response. Upon recognizing pathogens through receptors like Toll-like receptors (TLRs) and NOD-like receptors (NLRs), macrophages activate proteins such as TIRAP and RIPK2, leading to the production of pro-inflammatory cytokines. However, dysregulation of these pathways can result in a cytokine storm, causing tissue damage, organ failure, and potentially death. Macrophages are central to the inflammatory response, detecting pathogens via pattern recognition receptors like TLRs and NODs. Adaptor proteins such as TIRAP and RIPK2 mediate downstream signaling, leading to the production of pro-inflammatory cytokines. However, dysregulation of these pathways can result in a cytokine storm, causing tissue damage, organ failure, and potentially death.

1.2 Role of TIRAP and RIKP2 in inflammation

Macrophages play an important role in mediating inflammatory signaling. Several receptors present on them, such as TLRs and NOD, recognize PAMPs associated with bacteria. TIRAP and RIPK2 mediate the downstream signaling, thus producing pro-inflammatory cytokines. Upon recognition of pathogen-associated receptors (PRRs) such as Toll-like receptors (TLRs) and NOD-like receptors (NLRs), intracellular signaling cascades are initiated to trigger an immune response. TIRAP (Toll-

interleukin 1 receptor (TIR) domain containing adaptor protein) functions as a bridging adaptor that facilitates the recruitment of MyD88 to TLR2 and TLR4 upon detection of bacterial components like lipoproteins or lipopolysaccharide (LPS). This leads to the activation of downstream kinases, including IRAKs and TRAF6, which in turn activate the NF-κB and MAPK pathways, resulting in the transcription of pro-inflammatory cytokines. In parallel, RIPK2 (Receptor-interacting serine/threonine-protein kinase 2) is a key kinase downstream of NOD1 and NOD2, cytosolic receptors that recognize bacterial peptidoglycans. Upon activation, RIPK2 undergoes ubiquitination and recruits TAK1 and IKK complexes, leading to NF-κB activation and cytokine gene expression. Together, TIRAP and RIPK2 coordinate innate immune signaling from both surface and intracellular PRRs, amplifying the inflammatory response through the production of cytokines such as TNF-α, IL-1β, and IL-6. Thus, targeting them serves as an important therapeutic target to dampen chronic inflammation. Several critical residues (Proline 169, Phenylalanine 193, Methionine 194, and Tyrosine 195) reported for the interaction of TIRAP with the kinases BTK and Kinase C delta (PKCδ) are therapeutic site to stop phosphorylation of TIRAP, which is important for downstream signaling[5]. Also, on activation, RIPK2 auto-phosphorylates itself, which is essential for mediating pro-inflammatory cytokines. Inhibiting critical residues (47, 66, 94, 95, 96, 143, 144, 164, 165) on the kinase domain of RIPK2 results in the inhibition of phosphorylation and, thus, inhibition of chronic inflammation[6]**.**

1.3 *Withania somnifera* compounds as potent anti-inflammatory molecules

Withania somnifera, also referred to as Ashwagandha, is an evergreen shrub native to India, Nepal, the Middle East, and Africa. In traditional Ayurvedic medicine, Ashwagandha has been in use as a medicinal plant for thousands of years. *Withania somnifera* contains bioactive compounds, including

withanolides, alkaloids, and flavonoids, which have demonstrated anti-inflammatory properties in various studies. These compounds may help modulate the body's inflammatory response It has immunomodulatory effects, enhancing macrophage activity by increasing their phagocytic ability and proinflammatory cytokines production such as IL-6, IL-1β and TNF-α. It supports the immune response, promoting the elimination of pathogens and reducing inflammation[7]. Withania somnifera is known for its antioxidant properties, which can help neutralize free radicals and reduce oxidative damage and thus is effective in chronic inflammation associated with oxidative stress. This, in turn, may contribute to its anti-inflammatory effects. WS reduced the pro-inflammatory molecules levels and increased the anti-inflammatory molecules levels, suggesting its potential for treating inflammatory diseases caused by sleep deprivation[8]. Along with having anti-inflammatory properties, WS also alleviates other symptoms of pain associated with chronic inflammation. Although some studies have reported WS's anti-inflammatory properties, the mechanism is not fully understood yet and needs to be explored to use it for more effective treatment of chronic inflammation.

Chapter 2: Literature Review

2.1 Review of Past Work

Chronic inflammation driven by bacterial infections contributes majorly to the pathogenesis of several chronic inflammatory diseases. Both Gram-positive and Gram-negative bacteria can induce persistent inflammatory responses by activating innate immune pathways. Simultaneous targeting of TIRAP and RIPK2 will effectively reduce chronic inflammation by dampening both gram-positive and gram-negative bacteria-related chronic inflammation, respectively[9]. This strategy minimizes redundant and excessive activation of NF-κB, thereby reducing pro-inflammatory cytokine production and preventing macrophage hyperactivation[10]. Natural compounds are sought as anti-inflammatory agents due to their historical use, chemical diversity, and perceived safety. Traditional medicine systems have long employed natural remedies to treat inflammation because these compounds offer a broad spectrum of structures and properties, increasing the chances of finding effective anti-inflammatory agents. They are often considered safer to use because of fewer side effects, and suitable for long-term use in chronic conditions. In addition to that their antioxidant properties and immunomodulatory effects make them valuable in mitigating inflammation and oxidative stress[11]. *Withania somnifera* is a potent anti-inflammatory Indian medicinal plant having a plethora of chemical constituents such as steroidal lactones, flavonoids, phenolic compounds, saponins, alkaloids, etc.

2.2 Problem formulation and hypothesis

We hypothesize that certain bioactive compounds derived from WS will exhibit a modulatory effect on the interactions between TIRAP and key signaling molecules, BTK and the other one being PKCδ. Along with that, it will also inhibit the autophosphorylation of RIPK2 which will eventually lead to inhibition of downstream kinase activation[12]. Specifically, we

anticipate that the *Withania somnifera*-derived compounds' ability to disrupt or attenuate the TIRAP-BTK and TIRAP-PKCδ interactions and RIPK2 phosphorylation will effectively attenuate both the gram-positive and gram-negative bacteria-related chronic inflammation[13]. We further hypothesize that the anti-inflammatory mechanisms of these compounds will involve the inhibition of downstream signaling pathways associated with TIRAP and RIPK2, ultimately leading to a reduction in pro-inflammatory cytokines production and alleviating the inflammatory response[14]. Our research seeks to validate these hypotheses and identify lead compounds with therapeutic potential to treat diseases that are associated with chronic inflammation (Figure 1).

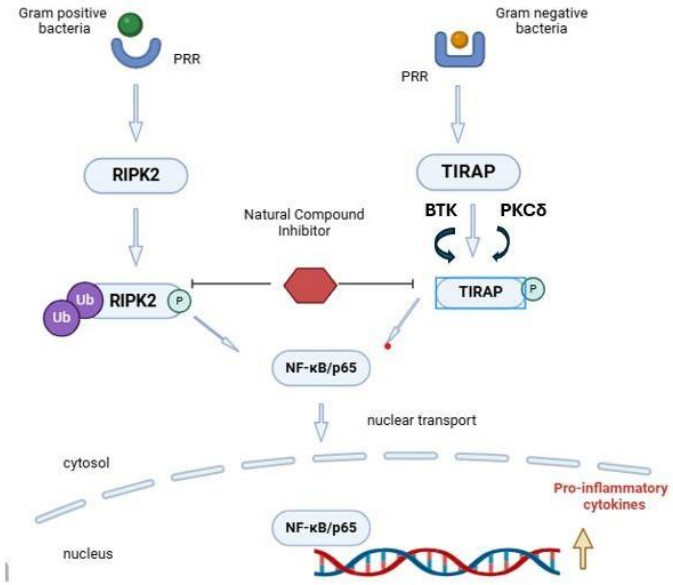

Figure 1: *Simultaneous targeting of TIRAP and RIPK2 for the treatment of chronic inflammatory disease (Created using Biorender).*

Chapter 3: Materials and Methods

3.1 Structure Data Retrieval and Preparation

The following protein receptor and ligand compounds were used for virtual screening against WS library compounds: TIRAP and RIPK2. The Crystal structure of human RIPK2 kinase domain in complex with ponatinib (PDB ID: 4C8B) with resolution 2.75 Å and the crystal structure of TIR domain of Mal/TIRAP (PDB ID: 3UB2) with resolution of 2.40 Å were retrieved from the RCSB PDB repository (https://www.rcsb.org/) and used for the study. The complexes were downloaded as a PDB file. The ligands were separated from the proteins, and water and heteroatoms were eliminated using BIOVIA Discovery Studio. Also, the structures using Amber ff14SB were minimized in the UCSF Chimera software for further studies.

For docking in the Schrödinger Suite's GLIDE module, receptors were prepared by using the Protein Preparation Wizard. The target proteins were refined, optimized at pH 7.0, and water molecules were removed. After that, it was minimized using the OPLS4 force field. Grid generation was done around the receptor by using the Receptor Grid Generation wizard, covering the entire protein structure.

For docking in AutoDock Vina, AutoDockTools-1.5.7 was used. The structure was converted into PDBQT format using AutoDockTools, and Kollman charges and polar hydrogens were added to the TIRAP protein. Blind docking was done by generating a Grid box covering the whole receptor.

3.2 Library Preparation

The computational library of *Withania somnifera* was prepared with 167 compounds it. Downloaded compounds from the PubChem database (https://pubchem.ncbi.nlm.nih.gov) and IMPPAT database (https://cb.imsc.res.in/imppat/home) in 3D conformation in SDF format.

The files were processed and further used for blind docking with RIPK2 and TIRAP targets in Maestro 13.1. For performing the blind docking in AutoDock Vina, the ligands were converted to a PDBQT file format by using Open Babel.

3.3 Molecular Docking and Virtual Screening:

The potential inhibitor site in TIRAP was identified at the interface where it interacts with both BTK and PKCδ, making it a prime target for drug screening. The interacting residues of TIRAP with the kinases BTK and PKCδ, within a 4Å distance, were analyzed using Chimera 1.13.1. It was observed that residues from the C-terminal region of TIRAP play a critical role in both interactions, leading to the selection of this region for virtual screening. Compounds from the *Withania somnifera* library, available in 3D SDF format, were processed and subjected to blind docking against the TIR domain of TIRAP using Auto Dock Vina. Docking scores were generated for each protein-ligand complex. To validate the preliminary results from AutoDock, Maestro was used to confirm ligand binding conformations. A similar approach was taken for RIPK2. The structures of TIRAP and RIPK2 were converted to a PDBQT file by using AutoDock tools, and docking grids were defined to fully encompass the protein structures. The ligand structures were also converted to PDBQT files using Open Babel. AutoDock Vina calculated the binding affinities in kcal/mol, with potential inhibitors being selected based on their interaction with the target site and a docking score of -5.0 or better. Visualization and analysis of the TIRAP-ligand interactions were performed using Discovery Studio Visualizer 2021. The workflow for identifying inhibitors targeting the TIRAP-BTK- PKCδ interface and the RIPK2 kinase domain from the *Withania somnifera* library is outlined in Fig. 2. Compounds that met the selection criteria on both docking platforms were further evaluated for ADMET properties to assess their pharmacokinetic profiles.

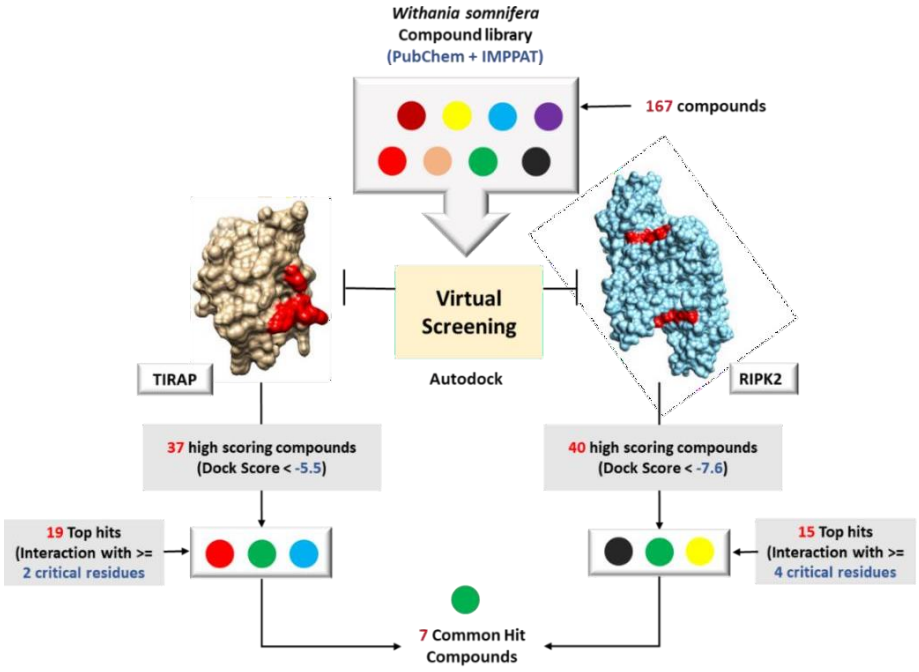

Figure 2: *Strategy of screening potent inhibitors against TIRAP and RIPK2 with Withania somnifera library* (*Created using BioRender*)

3.4 Physiological properties and ADMET predictions

The pharmacokinetics and ADMET properties of the selected compounds were analyzed on pkCSM server (https://biosig.lab.uq.edu.au/pkcsm/). The small molecule inhibitors that exhibited favorable physiochemical and ADMET properties were selected as potential therapeutic candidates to effectively inhibit the TIRAP and RIPK2 mediated pro-inflammatory NF-κB pathway.

3.5 Molecular dynamics (MD) simulation

To validate the stability of ligands within RIPK2 and TIRAP's active binding pocket, molecular dynamics (MD) simulations were conducted. The study used Gromacs 4.6, with extended simulations running for 200 ns. For topology generation, the Amber99sb-ildn force field was applied to macromolecules, while small molecules were prepared using the ANTECHAMBER module from AMBER Tools, tailored for Gromacs 4.6.The simulation setup involved placing either the Apo form of TIRAP

and RIPK2 (unbound) or their ligand-bound complexes at the center of a cubic simulation box, ensuring a minimum distance of 1.0 Å between the protein and the box edges. The systems were solvated with TIP3P explicit water molecules, as described by Jorgensen et al. (1983), and neutralized by introducing appropriate numbers of sodium or chloride ions, depending on the system's charge. Energy minimization was performed using the steepest descent method, followed by equilibration under constant volume (NVT) and constant pressure (NPT) conditions for 2 ns each, maintaining the pressure and temperature as 1 atm and 300 K, respectively. The resulting simulation trajectories were subsequently analyzed using Xmgrace to evaluate system stability and ligand behavior.

3.6 Mammalian Cell culture

RAW 246.7, which is a cell line of murine macrophages, was obtained from the cell repository of the NCCS, Pune, India. The cells were maintained in DMEM (supplemented with 10% (v/v) heat-inactivated fetal bovine serum, 100 U/ml penicillin, and 100 µg/ml streptomycin at 37ºC in a 5% CO_2 air humidified atmosphere. The cells were treated with 1000 ng/ml of LPS (L2630; Sigma), 2000 ng/ml of MDP (tlrl-mdp; InVivogen) for indicated time points.

3.7 MTT assay – In vitro Cytotoxicity Assessment

The viability of the cells (RAW 264.7) was checked in the presence of Quercetin and Kaempferol by a conventional MTT assay. The cells were seeded at approximately 4000 cells per well in 96-well plates containing 200 µL media and incubated at 37ºC in a 5% CO_2 for 24 hours. Following incubation, the old media was aspirated, and 100 µL of treatment media was added to each well, with incubation continued for an additional 24 hours. The drugs were checked for the concentration ranging from 1 to 50 µM. The wells containing only media were taken as control. After 24 hours, the media was replaced with fresh media containing 0.5 mg/ml MTT reagent.

The cells were further incubated for 4 hours at 37ºC. After that, the media was carefully aspirated, and the purple-colored formazan crystals were dissolved in 100 µL of DMSO per well. The absorbance was recorded at 570 nm, and the cell viability was calculated.

3.8 Quantitative reverse transcriptase PCR

To evaluate IL-1β, IL-6, and TNF-α gene expression, RAW 246.7 macrophages were treated as previously described. After that, the total RNA of the cells was extracted using TRIzol reagent (Invitrogen Life Technologies, Milan, Italy) according to the protocol provided by the manufacturer. The concentration of isolated RNA and its purity were determined using a nanodrop. For cDNA preparation, 1000 ng of RNA was reverse transcribed using the cDNA Synthesis Kit (6110A; Takara). The real-time qPCR was performed using SYBR green master mix (A25742; Applied Biosystems) in StepOnePlus RealTime PCR Systems (Applied Biosystems). The experiment was performed in three independent sets for the gene expression of GAPDH along with the pro-inflammatory cytokine genes.

3.9 Immunofluorescence

In 12-well culture plates, $1x10^4$ cells were cultivated on coverslips (18 mm in diameter). Overnight, all cells were grown in serum-free DMEM to allow them to synchronize. Cells were given drug treatment for 30 minutes prior to LPS treatment. Cells were then washed with 1x PBS once after the medium had been aspirated. The cells were fixed for 20 minutes at room temperature with freshly prepared 4% paraformaldehyde, and then, after washing, they were permeabilized for 15 minutes with 0.1% Triton-X 100. Cells were blocked with 5% BSA in 1X Tris-buffered saline, 0.1% Tween®20 detergent (TBST) for 60 minutes, after fixation and permeabilization, followed by an overnight staining procedure at 4°C using primary antibodies with a 1:200 dilution in blocking buffer. The cells were

stained with secondary antibodies at a dilution of 1:500 in 1X TBST for an hour at room temperature after being washed with TBST three times for 5 minutes each. Nuclear counterstaining, along with mounting, is carried out in accordance with the manufacturer's instructions using DAPI-containing mounting media. The Olympus confocal laser scanning microscope (FV100) was used to study the coverslips after mounting them onto glass slides with mounting fluid. Images were taken at 100X magnification. The list of primary antibodies and secondary antibodies are listed in **Table-5.2**.

Chapter 4: Results and Discussions

4.1 Virtual screening and analysis:

For the *in-silico* screening of potential drug compounds, blind docking of 167 compounds was performed from the WS library with the TIR domain of the TIRAP protein structure. We utilized the IMPPAT and PubChem database to prepare the library of these phytoconstituents for *in silico* screening. Potential compound candidates were screened, that possibly had the potential to block the site of TIRAP interaction with its activating and phosphorylating partners BTK and PKCδ to regulate the downstream inflammatory signaling in macrophages. The drug(compound library) and TIRAP blind docking were performed in the AutoDock. AutoDock Vina calculated the binding affinity (kcal/mol). The docked drug candidates were then arranged based on their docking score (high to low), and the compounds having docking scores above -5.5 (37 compounds) were studied in Discovery Studio Visualizer 2021. The top nineteen drug compounds that interacted with at least two critical residues of TIRAP had docking scores above -5.5. Furthermore, to reconfirm the drug docking, the blind docking of compounds was performed through another docking platform, Schrödinger Suite's GLIDE module. The docking results from aligned with the data of AutoDock Vina docking.

The same procedure was followed for RIPK2 docking with WS compound library. The blind docking of RIPK2 and drug was then performed in the AutoDock. AutoDock calculated the binding affinity of each compound with RIPK2 in kcal/mol. Arranged the docked compound candidates in descending order based on their docking score and the compounds having docking score above -7.6 (40 compounds) were studied in Discovery Studio Visualizer 2021. The top fifteen compounds that were interacting with a minimum of four critical residues of RIPK2 and had docking scores above -5.5 were selected. The top-scoring compounds were selected based on a docking score threshold determined by comparison with known inhibitors

(Dorzolamide for TIRAP and Ponatinib for RIPK2) ensuring that only compounds with superior binding affinity were considered. These selected hits were further analyzed to confirm whether they bound to the therapeutic site, with selection criteria based on the number of critical interacting residues.

Docking was performed in Schrödinger Suite's GLIDE module to validate the results. Seven compounds were obtained that were common in both TIRAP and RIPK2 docking. From them, the top four potent compounds were selected based on docking score and interaction with critical residues, as discussed on both platforms and with both TIRAP and RIPK2. This resulted in the selection of the following compounds: Quercetin, Kaempferol, Anaferine, and Scopoletin to have potent interaction-blocking activity of protein TIRAP with the kinases BTK and PKCδ and also blocking RIPK2 phosphorylation. The binding pose of Quercetin, Kaempferol, Scopoletin and Anaferine with the proteins TIRAP and RIPK2 are displayed in Figure 3.

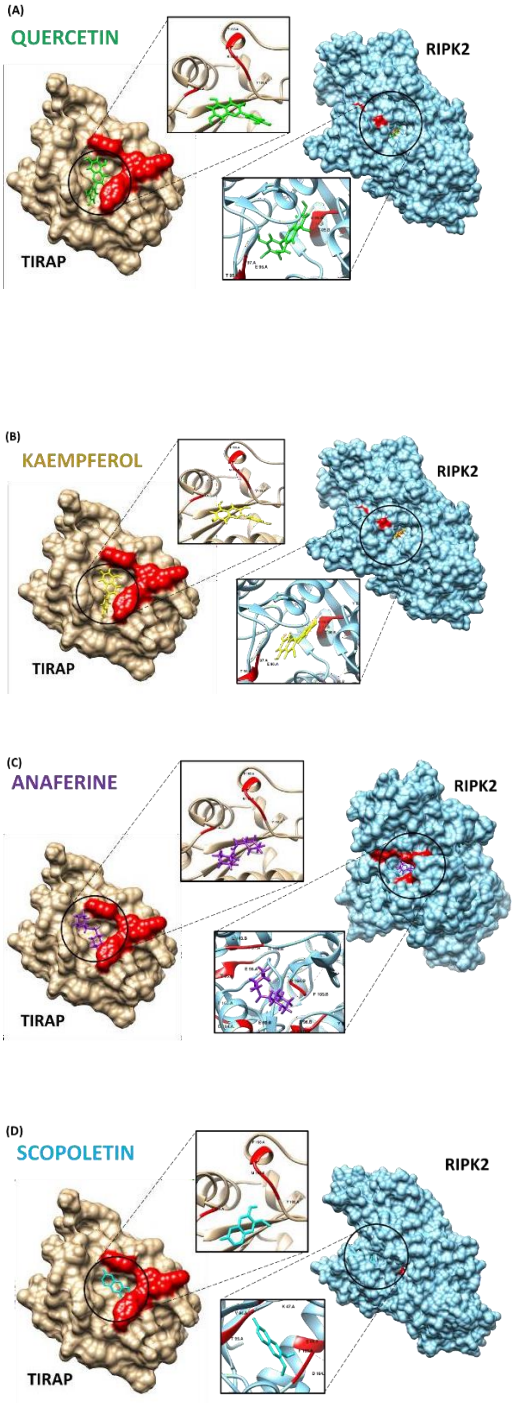

Figure 3: *3-D interaction pattern of each compound with TIRAP protein and RIPK2 (A) Quercetin (B) Kaempferol (C) Anaferine (D) Scopoletin*

The details of the selected compounds, their docking score in Maestro, bonding pattern and structure are presented in Table 1.

Table 1 Binding affinity of top-scored compounds common in TIRAP and RIPK2 screening

S.NO.	COMPOUND	PUBCHEM CID	TIRAP-WITANIA LIBRARY BINDING AFFINITY (kcal/mol)		RIPK2 –WITHANIA LIBRARY BINDING AFFINITY (kcal/mol)	
			AUTODOCK VINA	GLIDE	AUTODOCK VINA	GLIDE
1.	Quercetin	5280343	-7.6	-6.141	-11.1	-9.069
2.	Scopoletin	5280460	-6.0	-5.526	-10.2	-6.72
3.	Kaempferol	5280863	-7.5	-6.477	-8.9	-8.933
4.	Anaferine	443143	-6.3	-5.656	-8.1	-6.8

4.2. ADMET analysis of the virtually screened compounds

Poor pharmacokinetic profiles, encompassing absorption, distribution, metabolism, excretion (ADME), including toxicity, are the reason for the failure of approximately 90% of the drugs. The determination of ADMET properties is a means to evaluate the drug-likeness of chemical compounds along with their safety and efficacy and plays a critical role during drug discovery. A drug can be efficacious only if it has strong stable binding with the target protein, coupled with appropriate pharmacokinetic parameters.

Hence, the ADMET properties for the selected compounds were determined in-silico using pkCSM server (https://biosig.lab.uq.edu.au/pkcsm/) to preempt the failure of the drugs during pre-clinical and clinical phases. The pkCSM server leveraged both general properties of the compound and distance-based graph signatures for the prediction of ADMET attributes [15].

The selected compounds, namely Quercetin, Kaempferol, Anaferine, and Scopoletin, were screened for ADMET properties, and all the compounds showed appropriate physicochemical and ADMET properties, claiming the safety and efficacy of the compounds (Table 2). The physicochemical parameters evaluated encompassed molecular weight, lipophilicity,

rotatable bonds, acceptor bonds and donor bonds[16]. The compounds followed the rule of five for drug likeliness. Absorption parameters encompassed solubility in water, absorption in the intestine, CaCo2 permeability, and permeability to skin, and distribution parameters included central nervous system permeability, fraction unbound, and blood-brain permeability parameters. The values for absorption and distribution met the acceptable ranges. Notably, no substrates were found for CYP2D6 inhibitors or CYP2D6 substrates for selected compounds. The compounds exhibited non-toxic profiles with respect to hepatotoxicity, AMES toxicity and skin sensitization while Anaferine showed skin sensitization. These findings indicated the safety and efficacy of the selected compounds against the TIRAP. However, Anaferine cannot be used for topical application.

Furthermore, the selected compounds need to be validated in vitro and in vivo to harness their full therapeutic potential against TIRAP and RIPK2 receptor and their application in the treatment of various inflammatory diseases.

Table 2 ADMET properties of selected compounds

Parameters		Quercetin	Kaempferol	Anaferine	Scopoletin
Physicochemical Properties	M.W	302.238	286.239	224.348	192.17
	logP	1.988	2.2824	1.6199	1.5072
	Rotatable bond	1	1	4	1
	Acceptor bond	7	6	3	4
	Donor bond	5	4	2	1
Absorption	Water Solubility	-2.925	-3.04	-1.204	-2.504
	CaCo2 permeability	-0.229	0.032	1.336	1.184
	Intestinal absorption	77.207	74.29	93.738	95.277
	Skin Permeability	-2.735	-2.735	-3.337	-2.944
Distribution	Fraction unbound	0.206	0.178	0.754	0.363
	BBB Permeability	-1.098	-0.939	0.112	-0.299
	CNS Permeability	-3.065	-2.228	-3.249	-2.32
Metabolism	CYP2D6 substrate	No	No	No	No
	CYP2D6 inhibitor	No	No	No	No
Excretion	Total clearance	0.407	0.477	1.272	0.73
Toxicity	AMES Toxicity	No	No	No	No
	Hepatotoxicity	No	No	No	No
	Skin sensitization	No	No	Yes	No

4.3 MD Simulation data analysis:

MD simulation was performed to determine the stability of the protein-ligand complex, and docking complexes of the TIRAP and RIPK2 proteins with ligands were used as the initial system. An MD simulation of 200 ns was performed using the Gromacs 4.6 program. The RMSD analysis throughout the MD trajectory suggested no significant deviations and fluctuations in the complexes of all four TIRAP-ligand and RIPK2-ligand complexes (Fig. 4). Thus, we can infer that the complexes are stable as lower deviations can measure conformational stability. However, further *in vitro* studies are required to validate the results.

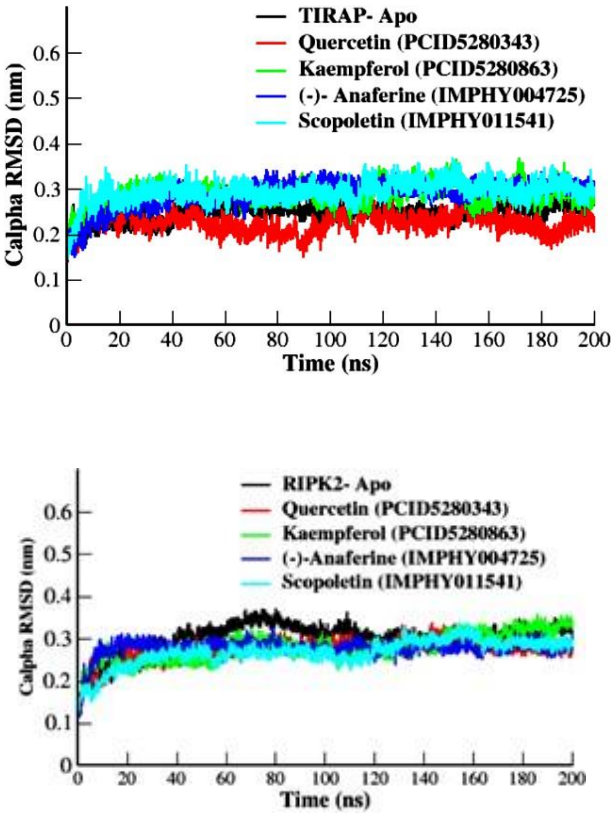

Figure 4: *Structural dynamics of TIRAP and RIPK2 complexes calculated over 200 ns of MD trajectories.*

4.4 Cell viability assay to assess the cytotoxic effects of the compounds:

To evaluate the cytotoxic or proliferative effects of the compounds on the cells, a comparative analysis of their impact on RAW 264.7 cells was conducted. Cells were treated with varying concentrations of the compounds, ranging from 1 µM to 50 µM, and incubated for 24 hours, followed by cell viability assessment. No significant differences in viability were observed between the control group and cells treated with up to 50 µM of the compounds. Based on these findings, concentrations up to 50 µM were considered non-cytotoxic and were selected for subsequent experiments (Fig. 5).

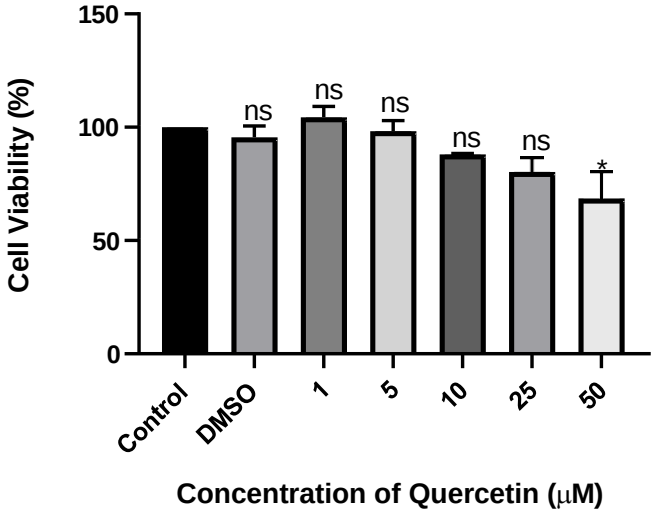

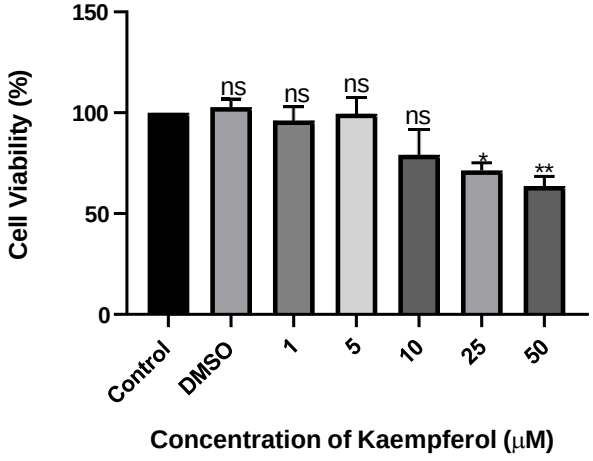

***Figure** 5: Effect of Quercetin and Kaempferol on cell viability. The cytotoxicity of Quercetin and Kaempferol on the viability of RAW 264.7 cells was determined using MTT analysis. The cells were treated with the indicated compound for 24 hr at varied concentrations (i.e., 1, 5, 10, 25 and 50 μM). All data are representative of three independent experiments and are presented as the mean ± SD, (One-way Anova test). **P = 0.001; *P = 0.01.*

4.5 Effect of Quercetin and Kaempferol on Inflammatory Gene Transcription:

The anti-inflammatory properties of Quercetin and Kaempferol were accessed by evaluating the mRNA levels of pro-inflammatory cytokines, TNF-α, IL-1β, and IL-6 by quantitative real-time PCR. The Quercetin treatment in LPS-stimulated cells showed a decrease in all three above-mentioned cytokines (Fig. 6). The drug's effect on the expression of these cytokines was also evaluated. The drug alone had almost negligible effects on the basal level expression of these cytokines as compared to the control.

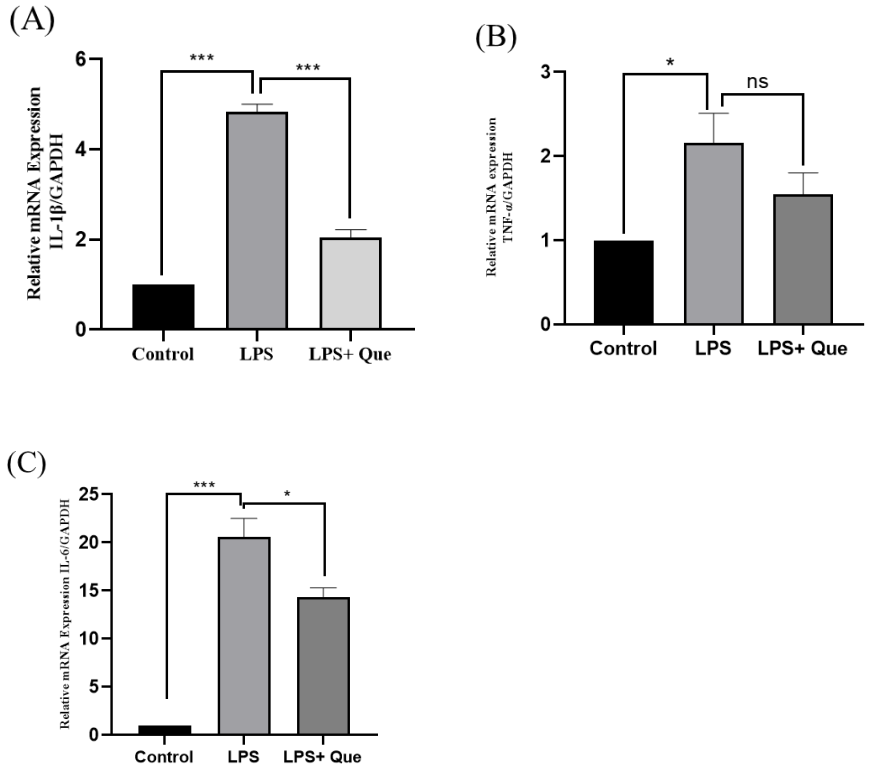

Figure 6: *The mRNA expression levels of pro-inflammatory cytokines (a) IL-1β, (b) TNF-α, and (c) IL-6 in RAW 264.7 macrophages in response to LPS (1000 ng/ml) to check the effect of Quercetin (10 µM). All data are representative of three independent experiments and are presented as the mean ± SD (One-way Anova test). ****P= 0.00001; ***P= 0.0001; **P = 0.001; *P = 0.01.*

Similarly, LPS-stimulated cells treated with Kaempferol showed a significant decrease in the pro-inflammatory cytokines concentration 10µM. (Fig 7)

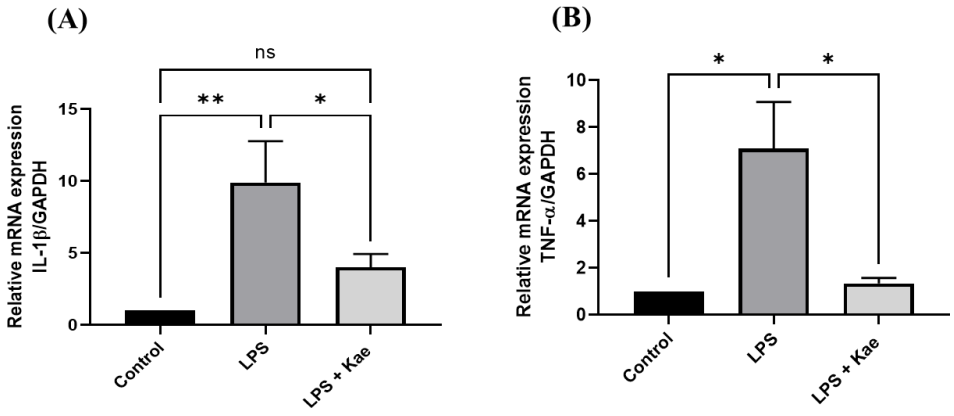

Figure 7: *The mRNA expression levels of pro-inflammatory cytokines (a) IL-1β, (b) TNF-α in RAW 264.7 macrophages in response to LPS (1000 ng/ml to check the effect of Kaempferol (10 µM). All data are representative of three independent experiments and are presented as the mean ± SD, (One-way Anova test). **P = 0.001; *P = 0.01.*

Further, to check the effect of Quercetin on the RIPK2-mediated inflammatory pathway. RAW 264.7 cells were stimulated with MDP to induce the pro-inflammatory response. MDP-stimulated cells showed a significant increase in pro-inflammatory cytokines, whereas cytokine expression decreased on treatment with 1µM Quercetin (Fig. 8). Similarly, MDP stimulated RAW 264.7 cells also showed a significant decrease in pro-inflammatory cytokines expression levels on treatment with Kaempferol (Fig. 9)

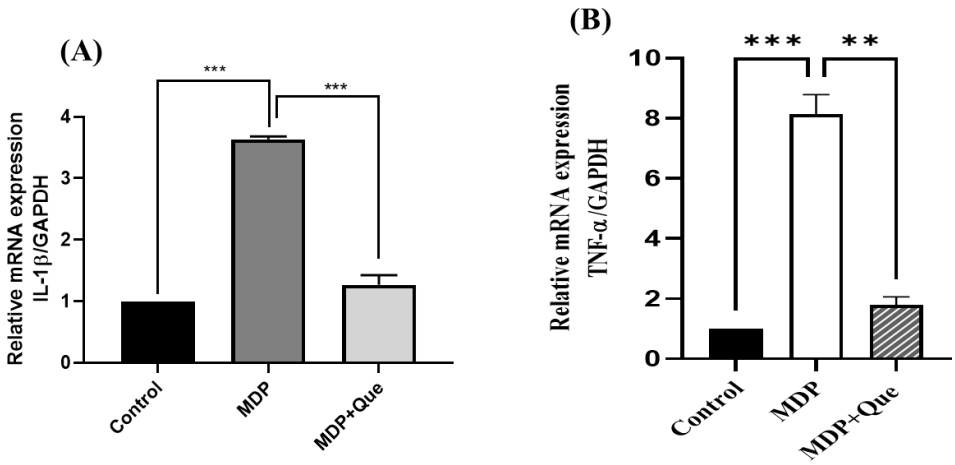

Figure 8: *The mRNA expression levels of pro-inflammatory cytokines (a) IL-1β, (b) TNF-α in RAW 264.7 macrophages in response to MDP (2000 ng/ml to check the effect of Quercetin (10 µM). All data are representative of three independent experiments. ***P= 0.0001; **P = 0.001; *P = 0.01*

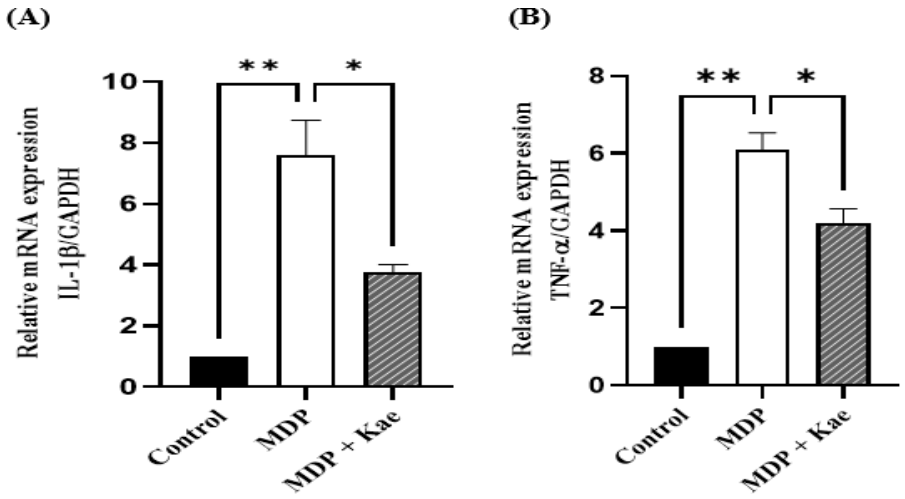

Figure 9: *The mRNA expression levels of pro-inflammatory cytokines (a) IL-1β, (b) TNF-α in RAW 264.7 macrophages in response to MDP (2000 ng/ml to check the effect of Kaempferol (10 µM). All data are representative of three independent experiments. **P = 0.001; *P = 0.01*

4.6 Compounds inhibit TIRAP phosphorylation in LPS-stimulated macrophages.

Upon LPS stimulation of macrophages, TLR4 and TIRAP are phosphorylated by kinases. Tyrosine phosphorylation of the TIRAP TIR domain is crucial for its downstream activity. Because the in-silico analysis suggested that both the compounds i.e. Quercetin and Kaempferol interacts with TIRAP, it was predicted that treatment with these compounds would decrease TIRAP phosphorylation. Both Y86 and Y106 within the TIRAP TIR domain represent crucial phosphorylation sites for PKCδ. Phosphorylation of TIRAP at Y86 (p-TIRAP) showed a modest increase over time, significantly decreasing this at post-LPS treatment in drug-treated RAW 264.7 macrophages. No changes in total TIRAP levels were observed. However, the downregulation of TIRAP phosphorylation at LPS activation strongly suggests that drugs decrease TIRAP activation by blocking its interaction with PKCδ and subsequent phosphorylation by this kinase. Therefore, these data indicate that Kaempferol and Quercetin interact with TIRAP and might inhibit the downstream pro-inflammatory signaling (Fig. 10 and Fig. 11 respectively)

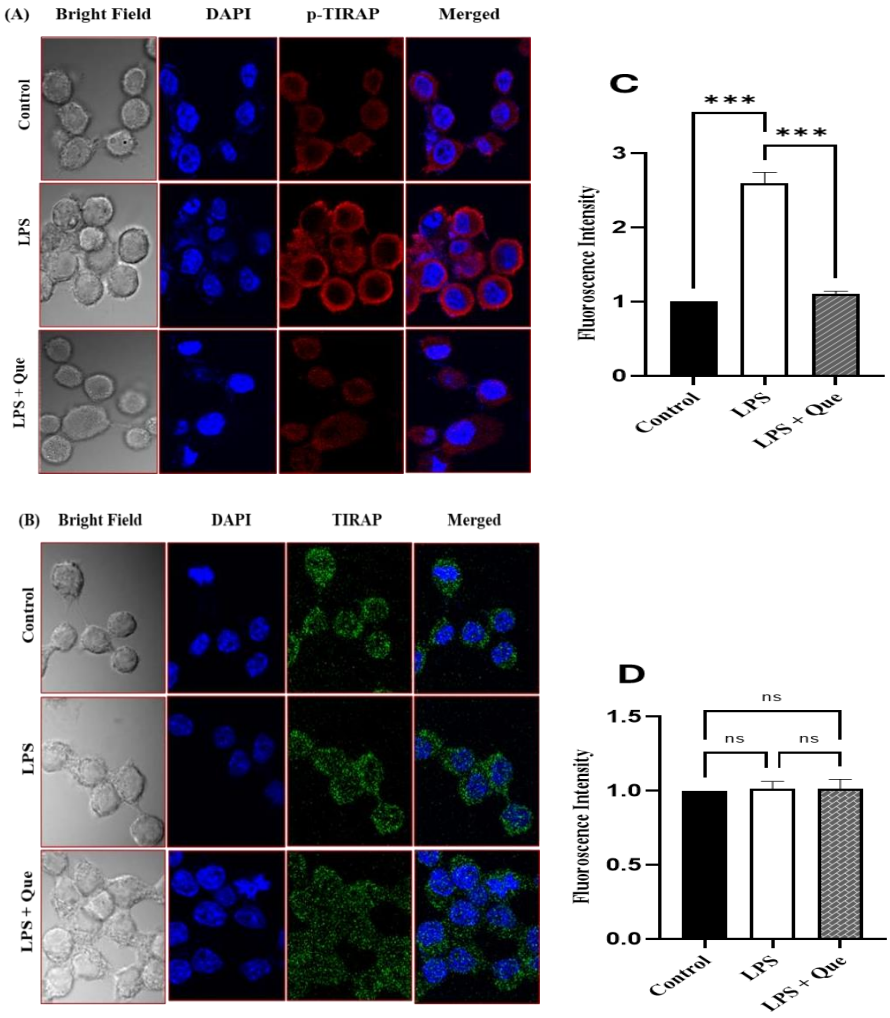

Figure 10: *Quercetin suppresses LPS-induced phosphorylation of TIRAP in RAW 264.7 macrophages. (A) Immunofluorescence confocal microscopy of p-TIRAP in RAW 264.7 macrophages. RAW 264.7 macrophages were treated with an anti-p-TIRAP antibody to determine the level of p-TIRAP (red). Nuclei were counterstained with DAPI (blue), and slides were visualized at 100x using confocal microscopy. Merged images of the red and blue fluorescence are shown. The images are representative of three independent preparations. (B) Immunofluorescence confocal microscopy of p-TIRAP in RAW 264.7 macrophages. RAW 264.7 macrophages were treated with an anti-TIRAP antibody to determine the level of TIRAP (green). Nuclei were counterstained with DAPI (blue), and slides were visualized using confocal microscopy. Merged images of the green and blue fluorescence are shown. The images are representative of three independent preparations. (C) and (D) Graphical representation of immunofluorescence confocal microscopy of p-TIRAP and TIRAP respectively. All data are representative of three independent experiments and are presented as the mean ± SD (One-way Anova test). ***P= 0.0001; **P = 0.001; *P = 0.01*

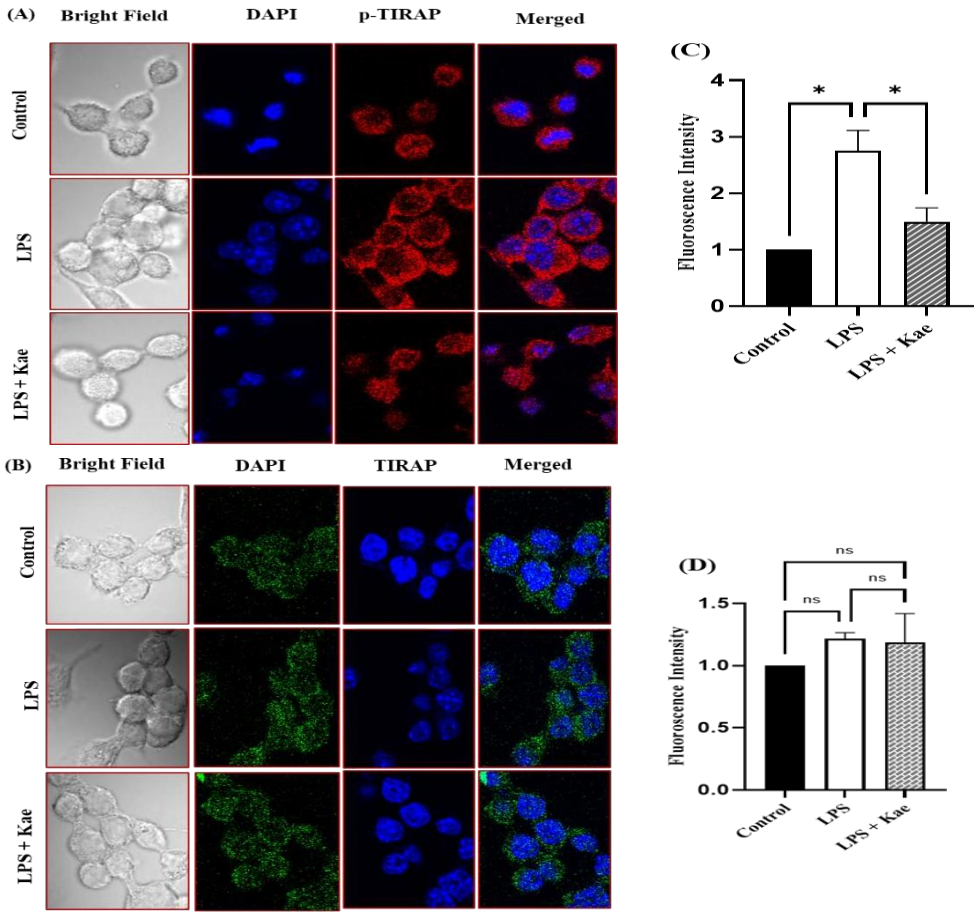

Figure 11: *Kaempferol suppresses LPS-induced phosphorylation of TIRAP in RAW 264.7 macrophages. (A) Immunofluorescence confocal microscopy of p-TIRAP in RAW 264.7 macrophages. RAW 264.7 macrophages were treated with an anti-p-TIRAP antibody to determine the level of p-TIRAP (red). Nuclei were counterstained with DAPI (blue), and slides were visualized at 100x using confocal microscopy. Merged images of the red and blue fluorescence are shown. The images are representative of three independent preparations. (B) Immunofluorescence confocal microscopy of p-TIRAP in RAW 264.7 macrophages. RAW 264.7 macrophages were treated with an anti-TIRAP antibody to determine the level of TIRAP (green). Nuclei were counterstained with DAPI (blue), and slides were visualized using confocal microscopy. Merged images of the green and blue fluorescence are shown. The images are representative of three independent preparations. (C) and (D) Graphical representation of immunofluorescence confocal microscopy of p-TIRAP and TIRAP, respectively. All data are representative of three independent experiments and are presented as the mean ± SD (One-way Anova test). *P = 0.01*

Chapter 5: Conclusion and Future Directions:

Our integrated study demonstrates that Quercetin and Kaempferol are novel and potent inhibitors of both TIRAP and RIPK2—two key mediators in inflammatory signaling. Through an in-silico screening of the *Withania somnifera* library, followed by 200 ns molecular dynamics simulations, we observed that these compounds effectively disrupt the interactions between TIRAP and the kinases BTK and PKCδ, as well inhibit RIPK2. This disruption interferes with the phosphorylation of TIRAP in LPS-stimulated macrophages and consequently leads to a marked reduction in the transcription of inflammatory genes. While previous studies have reported the inhibitory effects of Quercetin and Kaempferol on NF-κB, AP-1, and MAPK pathways, our work introduces a novel mechanism wherein these compounds target both TIRAP-dependent and RIPK2-mediated pathways, thereby dampening macrophage-driven inflammatory responses.

Looking ahead, further mechanistic studies are essential to delineate the precise molecular interactions disrupted by quercetin and kaempferol, including advanced binding analyses and extended molecular dynamics simulations. In vivo validation using appropriate animal models will also be critical to establish the pharmacokinetics, bioavailability, and safety profiles of these promising compounds. Additionally, while quercetin and kaempferol emerged as the most potent inhibitors in our screening, future investigations into the second-tier hits, such as Anaferin and Scopoletin, could provide insights into potential synergistic effects or alternative inhibitory mechanisms. Collectively, these findings set the stage for the development of targeted therapeutic strategies aimed at modulating TIRAP and RIPK2 activity to combat chronic inflammatory diseases.

APPENDIX-A

5.1 List of primers

Table 1 *Primer (mouse) sets used for RT-PCR*

S.No.	Target gene	Sequence (5´-3´)	T_m (°C)
1.	GAPDH (F)	AAT GTG TCC GTC GTG GAT CT	56.2
2.	GAPDH (R)	CCC TGT TGC TGT AGC CGT AT	57.1
3.	IL-1β (F)	TGG ACC TTC CAG GAT GAG GAC A	59.7
4.	IL-1β (R)	GTT CAT CTC GGA GCC TGT AGT G	57.1
5.	IL-6 (F)	CGC TAT GAA GTT CCT CTC TGC	55.3
6.	IL-6 (R)	CTA GGT TTG CCG AGT AGA TCT	54.4
7.	TNF-α (F)	GCC TCT TCT CAT TCC TGC TTG	55.9
8.	TNF-α (R)	CTG ATG AGA GGG AGG CCA TT	56.5

5.2 List of antibodies

Table 2 *Antibodies used for immunofluorescence.*

S. No.	Antibody	Cat. No.	Dilutions for immunofluorescence
1.	p-TIRAP	BS-756R	(1:200)
2.	TIRAP	13077S	(1:200)
3.	Anti-Mouse HRP	Sc-2318	(1:1000)
4.	Anti-Rabbit-AF594	A11012	(1:1000)

REFERENCES

1. Baig MS, Thurston TLM, Sharma R, et al. Editorial: Targeting signalling pathways in inflammatory diseases. *Front Immunol*. 2023;14:1241440. doi:10.3389/fimmu.2023.1241440

2. Peña OA, Martin P. Cellular and molecular mechanisms of skin wound healing. *Nat Rev Mol Cell Biol*. 2024;25(8):599-616. doi:10.1038/s41580-024-00715-1

3. Mekhael O, Revill SD, Hayat AI, et al. Myeloid-specific deletion of activating transcription factor 6 alpha increases $CD11B^{+}$ macrophage subpopulations and aggravates lung fibrosis. *Immunol Cell Biol*. 2023;101(5):412-427. doi:10.1111/imcb.12637

4. Nathan C, Ding A. Nonresolving Inflammation. *Cell*. 2010;140(6):871-882. doi:10.1016/j.cell.2010.02.029

5. Rajpoot S, Kumar A, Gaponenko V, et al. Dorzolamide Suppresses PKCδ -TIRAP-p38 MAPK Signaling Axis to Dampen the Inflammatory Response. *Future Med Chem*. 2023;15(6):533-554. doi:10.4155/fmc-2022-0260

6. Canning P, Ruan Q, Schwerd T, et al. Inflammatory Signaling by NOD-RIPK2 Is Inhibited by Clinically Relevant Type II Kinase Inhibitors. *Chem Biol*. 2015;22(9):1174-1184. doi:10.1016/j.chembiol.2015.07.017

7. Alanazi HH, Elfaki E. The immunomodulatory role of withania somnifera (L.) dunal in inflammatory diseases. *Front Pharmacol*. 2023;14:1084757. doi:10.3389/fphar.2023.1084757

8. Sri Ramachandra Medical College, Porur, Chennai, Tamil Nadu, India, Suganya K. Regulation of pro and anti-inflammatory signaling molecules in effect of Withania Somnifera root extract treated sleep deprivation induced Wistar rats. *Bioinformation*. 2020;16(11):856-862. doi:10.6026/97320630016856

9. Rajpoot S, Wary KK, Ibbott R, et al. TIRAP in the Mechanism of Inflammation. *Front Immunol*. 2021;12:697588. doi:10.3389/fimmu.2021.697588

10. Abbott DW, Yang Y, Hutti JE, Madhavarapu S, Kelliher MA, Cantley LC. Coordinated Regulation of Toll-Like Receptor and NOD2

Signaling by K63-Linked Polyubiquitin Chains. *Mol Cell Biol*. 2007;27(17):6012-6025. doi:10.1128/MCB.00270-07

11. Guo Q, Jin Y, Chen X, et al. NF-κB in biology and targeted therapy: new insights and translational implications. *Signal Transduct Target Ther*. 2024;9(1):53. doi:10.1038/s41392-024-01757-9

12. Moreira LO, El Kasmi KC, Smith AM, et al. The TLR2-MyD88-NOD2-RIPK2 signalling axis regulates a balanced pro-inflammatory and IL-10-mediated anti-inflammatory cytokine response to Gram-positive cell walls. *Cell Microbiol*. 2008;10(10):2067-2077. doi:10.1111/j.1462-5822.2008.01189.x

13. Canning P, Ruan Q, Schwerd T, et al. Inflammatory Signaling by NOD-RIPK2 Is Inhibited by Clinically Relevant Type II Kinase Inhibitors. *Chem Biol*. 2015;22(9):1174-1184. doi:10.1016/j.chembiol.2015.07.017

14. Nachbur U, Stafford CA, Bankovacki A, et al. A RIPK2 inhibitor delays NOD signalling events yet prevents inflammatory cytokine production. *Nat Commun*. 2015;6(1):6442. doi:10.1038/ncomms7442

15. Norinder U, Bergström CAS. Prediction of ADMET Properties. *ChemMedChem*. 2006;1(9):920-937. doi:10.1002/cmdc.200600155

16. Hodgson J. ADMET—turning chemicals into drugs. *Nat Biotechnol*. 2001;19(8):722-726. doi:10.1038/90761